Measuring the Film Thickness Surrounding a Bubble inside a Capillary

JING-DEN CHEN

Schlumberger-Doll Research Center, Old Quarry Road, Ridgefield, Connecticut 06877-4108

Received April 11, 1985; accepted June 10, 1985

The aqueous wetting film thickness surrounding a bubble (air or oil) inside a horizontal capillary tube is measured when the bubble is either stationary or moving at a constant speed v. A wide range of flow rates are covered in the measurements: $Ca \approx 10^{-7}$ to 10^{-4} for an air bubble, and $Ca \approx 10^{-6}$ to 10^{-3} for an oil bubble. The capillary number Ca is defined as $\mu_c v/\gamma$, where μ_c is the viscosity of the continuous liquid and γ the interfacial tension. Three different oils were used with oil-to-water viscosity ratio μ_b/μ_c = 0.51, 1.08, and 4.35. The wetting film thickness decreases as the bubble speed decreases until it approaches a constant value. Evidence is presented which suggests that the value of the constant is due to the roughness of the tube wall. For an air bubble moving at $Ca \approx 5 \times 10^{-5}$ to 3×10^{-4}, the measured wetting film thickness h correlates with the simple formula $h = 0.5rCa^{1/2}$, proposed by Fairbrother and Stubbs (*J. Chem. Soc.* **1**, 527, 1935). While for an oil bubble moving at $Ca \approx 2 \times 10^{-4}$ to 2×10^{-3}, the data agree better with $h = 1.337rCa^{2/3}$, a relationship derived by Bretherton (*J. Fluid Mech.* **10**, 166, 1961). There is no appreciable difference in the film thickness for the different oils for all Ca, its value being smaller than that for an air bubble moving at the same $Ca > 10^{-5}$.

1. INTRODUCTION

In this paper we report on experimental studies of the wetting film surrounding a bubble in a cylindrical capillary tube. The problem of a wetting film on a solid surface is of interest in connection with the distribution and flow of immiscible fluids in porous media and their electrical properties. During the waterflooding of oil in a water-wet porous medium, the aqueous wetting film on the solid surface can make the oil ganglia mobilization easier due to its lubricating effect but it can also have an adverse effect by breaking up the oil into small ganglia through a so-called snap-off mechanism (1–6).

The existence of a wetting film on a solid surface has a direct relation to the electrical conductivity since it provides an electrical path on an otherwise nonconducting solid surface. Electrical resistivity measurement of oil-bearing rock is used to estimate the water saturation, the fraction of void volume of a porous rock occupied by water. For the same water saturation, the resistivity of a rock is higher when water is the nonwetting phase than when it is the wetting phase (7–9). At low water saturations this contrast is even more remarkable. The lower resistivity exhibited by the water-wet rock has been attributed to the existence of a continuous water film, which provides an electrical path on an otherwise nonconducting solid surface (7).

Here we are interested in a much simpler geometry than the pores of a rock. We measured the wetting film thickness surrounding a moving or stationary bubble of air or oil in a cylindrical capillary tube.

Several studies have been done. Fairbrother and Stubbs (10) studied the relationship between the mean velocity v_m of a liquid in a capillary and the velocity v of an entrained air bubble. They found a simple empirical relationship

$$W \equiv \frac{v - v_m}{v} = Ca^{1/2} \quad \text{for}$$

$$7.5 \times 10^{-5} < Ca < 0.014 \quad [1]$$

for bubbles with length larger than three times the radius r of the capillary. Assuming that the

0021-9797/86 $3.00

liquid film surrounding the bubble was at rest with respect to the tube, they derived

$$\frac{W}{2} = \frac{h}{r} = 0.5Ca^{1/2}, \qquad [2]$$

where h is the thickness of the film surrounding the bubble, and Ca the capillary number. Ca is defined as $\mu_c v/\gamma$, where μ_c is the viscosity of the continuous liquid and γ the interfacial tension.

By measuring the fraction of liquid left on the wall of a tube when expelled by air, Taylor (11) extended the validity of Eq. [2] for Ca up to 0.09.

Kussakov and Mekenitskaya (12) measured conductimetrically the average thickness of an aqueous electrolyte film surrounding an apparently stationary gas or oil bubble inside a glass or quartz capillary. Thicknesses of equilibrium film of the order of 100 to 10,000 Å in capillaries of 0.03 to 0.13 cm radii were measured and the rupture of the film was detected by the sudden decrease in electrical conductivity to an unmeasurable extent.

Marchessault and Mason (13) measured the film thickness conductimetrically and found a good agreement with Eq. [2]. They also proposed a relation

$$\frac{h}{r} = -0.05\left(\frac{\mu_c}{\gamma}\right)^{1/2} + 0.89Ca^{1/2}. \qquad [3]$$

About 1 decade of Ca (7×10^{-6} to 2×10^{-4}) was covered in their experiments.

Making use of the lubrication theory and assuming there is no tangential stress at the fluid–fluid interface, Bretherton (14) predicted that

$$\frac{h}{r} = 1.337Ca^{2/3} \qquad [4]$$

was accurate within 5% error if $Ca < 0.003$ and 10% error if $Ca < 0.005$. By measuring the change in length of a liquid slug moving at a constant speed inside a tube for a certain distance, he calculated the fraction of liquid left on the wall of the tube. His experimental data showed good agreement with Eq. [4] for $Ca \approx 10^{-3}$ to 10^{-2}, but a systematic deviation for $Ca \approx 10^{-6}$ to 10^{-3}. For $Ca < 10^{-3}$, his theory underestimated the data while Eqs. [2] and [3] overestimated. He discussed the possible reasons for the deviation, such as the roughness of the tube, rigid fluid–fluid interface, and the disjoining pressure. But no satisfactory explanation was reached.

Goldsmith and Mason (15) measured the film thickness h surrounding a moving bubble through a microscope and found good agreement with Eq. [2] for bubbles with negligible viscosity μ_b compared to that of the continuous phase μ_c for $0.013 < Ca < 0.09$. They also found the film to be at rest for these bubbles in this range of Ca. The data began to deviate from Eq. [2] for $Ca > 0.1$, which is consistent with Taylor's observation. Unfortunately, the smallest Ca of their experiments (their system 6a) is 0.013, which is too large to check the validity of Eq. [4].

Teletzke (16) studied theoretically the displacement of one fluid by another in a tube and found that at high Ca, when the disjoining pressure was negligible, the h–Ca relation was the same as Bretherton's result, and that at low Ca, when the disjoining pressure was effective, a wetting film might or might not exist depending on the disjoining pressure (for more details on wetting films, see (2, 16–18) and references therein).

2. EXPERIMENTAL

Figure 1 shows a sketch of the experimental set-up. Plexiglas chambers, A, are connected to each end of a precision bore glass capillary tube, C, 0.04064 cm in radius and 25.4 cm long (Wilmad Glass Co.). After the cleaning procedure described below, both chambers and tube are filled with the conducting liquid injected from a syringe connected to the left chamber through Teflon tubing. The right chamber is connected to another filled syringe through a Teflon tube after a bubble, B, of certain length is introduced into the tube through this chamber using a microsyringe.

The bubble is forced to move to the left end of the tube by injecting the conducting liquid

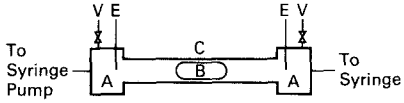

FIG. 1. Sketch of experimental setup: A, Plexiglas chambers; B, bubble; C, capillary tube; E, electrodes; V, valves.

from the right syringe with the valve, V, on the left chamber open. The valve is then closed and the one on the right opened. Both the speed v and electrical resistance R_b measurements were made when the bubble is being pushed by a constant volumetric flux of conducting liquid delivered from the left syringe by a constant flow rate pump. The flow is stopped before the bubble reaches the right end of tube. The same bubble can be used many times by repeating the procedure just described until a complete set of experiments are done for the fluid system. Before each set of experiments, the tube was cleaned with distilled water, acetone, and chromic acid, and then rinsed with distilled water and finally with the conducting liquid. The speed of moving bubble can be varied by changing the pump gear and the syringe size and is determined by measuring the time spent for the bubble to travel a predetermined distance.

The electrical resistance across the tube is monitored and recorded at suitable time intervals using a Hewlett–Packard LCR meter. The meter is connected to two silver wires, E, which are inserted into the Plexiglas chambers, A, and dipped in the conducting liquid. The electrical resistance can be measured at three frequencies, 120, 1000, and 10,000 Hz. For the range of resistance, 0.2 to 2.5 MΩ, the measured value increases asymptotically with decreasing frequency but the difference between those at 120 and 1000 Hz is no more than 2% of the measured value. All electrical measurements were made at 1000 Hz. During the experiment, the tube was set horizontally.

The conducting liquid used was 0.1 N NaOH aqueous solution received from Crescent Chemical Company. It has a conductivity k of 0.0204 $(\Omega\ \text{cm})^{-1}$. The concentration of NaOH is high enough to eliminate the effect of surface conductivity. The oils used were Soltrol 10, 100, and 220 from Phillips Chemical Company. To improve the visualization, the oils were dyed red (1 mg of Oil Red O in 1 ml of oil). The fluid properties are listed in Table I and the relevant properties given are for dyed oil. The viscosities were measured using a capillary viscometer, the densities by Mettler digital density meter, and the interfacial tension by the sessile drop method. The experiments were run at room temperature (22.5 to 23.8°C).

3. RESULTS AND DISCUSSION

Depending upon the initial film thickness and the flow rate, the electrical resistance R_b decreases or increases monotonically until it reaches an apparent "steady" value for that specific flow rate. The higher the flow rate, the quicker this value is reached, from about a second to about 20 min. This means that the distance traveled by the bubble is about three times its length before the steady value is reached. But due to the imperfection of the capillary tube, after this steady value is reached, some variation of R_b was observed as the bubble moves through the capillary. The range of variation was larger for slower bubble speed. A maximum value of 3% of the mean value was measured for the highest flow rate, while a value of 40% was measured for the lowest flow rate. This percentage represents the difference between the maximum and minimum values of R_b divided by their mean

TABLE I

Fluid Properties

	γ (dyn/cm)	μ (cp)	ρ (gm/cm^3)	μ_b/μ_c
Air	70	0.0098[a]		0.01
Soltrol 10	11.2	0.49	0.69	0.51
Soltrol 100	10.6	1.05	0.74	1.08
Soltrol 220	11.5	4.22	0.79	4.35
0.1 N NaOH	—	0.97	1.00	—

[a] Taken from handbook for saturated water vapor at 21°C.

value. For the data presented in Table II, R_b has a mean of 0.55 MΩ with a standard deviation of 0.02 MΩ at the highest flow rate and it has a mean of 1.79 MΩ with a standard deviation of 0.21 MΩ at the lowest flow rate. Plots of R_b against sampling time for low flow rates showed the same pattern of variation when the experiment was repeated. We used another tube but had the same problem. And the second tube had its own pattern of variation in the plot of measured R_b vs its length. This indicates the variation is due to the imperfection of capillary tube.

We then decided to examine the tube. The cross section of the tube was found to be circular. We measured the tube diameter through an optical microscope on the central portion of the tube and found a variation of 0.7% in diameter over a length of 7.5 cm. This is not significant enough to account for the 40% variation in R_b when the bubble was moving slowly through the tube. Two sections of the tube were examined under an electron microscope. Few small scratches and many axially directed grooves with varying width of less than 10 μm on the inside surface of the tube were seen through a scanning electron microscope. These grooves are neither perfectly parallel to each other nor of the same width, as shown in Fig. 2. We were not able to measure the depth of these grooves accurately due to the chipping of tube wall from griding on the cross section. But it is estimated to be less than 1 μm. From these observations, we believe that the variation is mostly due to these grooves.

For each flow rate we calculate the film thickness for the maximum, the minimum, and the mean values of R_b using the equation (13)

$$h = \frac{L}{2\pi r k(R_b - R_0)}, \qquad [5]$$

where L is the film length, r tube radius, k conductivity of aqueous solution, R_b and R_0 electrical resistance across the tube with and without the bubble. For the tube and

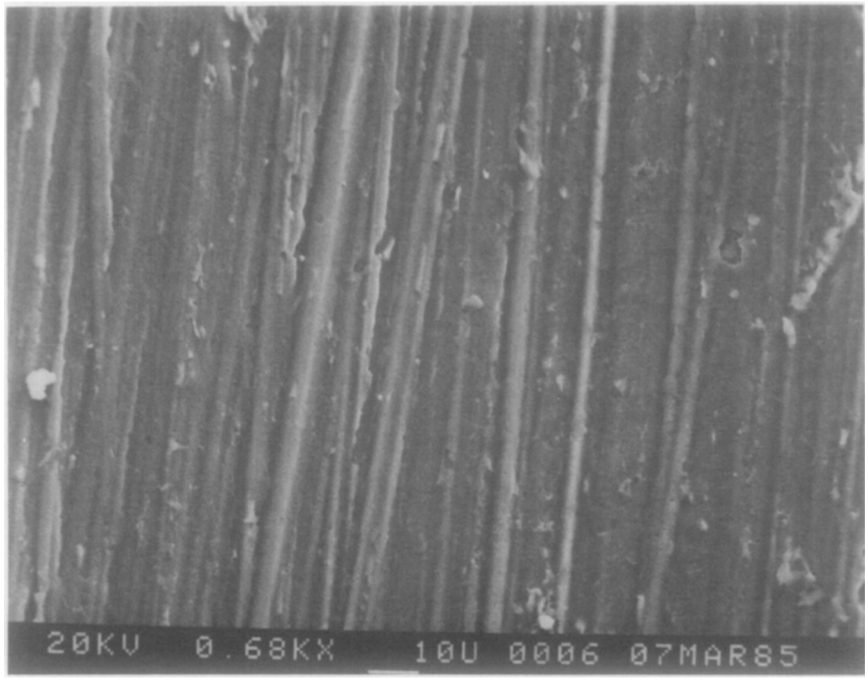

FIG. 2. An SEM micrograph showing the axially directed grooves on the tube wall. The bar scale at the bottom is equal to 10 μm.

TABLE II

Experimental Data for Air Bubble, $L = 0.603$ cm

v (cm/s)	Ca	h_{max} (cm)	h_{min} (cm)	h (cm)	$\frac{h}{r}$
1.95	2.74×10^{-4}	3.76×10^{-4}	3.53×10^{-4}	3.61×10^{-4}	8.88×10^{-3}
1.39	1.93×10^{-4}	3.43×10^{-4}	2.91×10^{-4}	3.12×10^{-4}	7.68×10^{-3}
0.97	1.34×10^{-4}	2.71×10^{-4}	2.37×10^{-4}	2.51×10^{-4}	6.18×10^{-3}
0.715	9.91×10^{-5}	2.24×10^{-4}	1.97×10^{-4}	2.10×10^{-4}	5.17×10^{-3}
0.523	7.25×10^{-5}	1.87×10^{-4}	1.71×10^{-4}	1.79×10^{-4}	4.40×10^{-3}
0.362	5.02×10^{-5}	1.64×10^{-4}	1.40×10^{-4}	1.51×10^{-4}	3.71×10^{-3}
0.269	3.73×10^{-5}	1.45×10^{-4}	1.23×10^{-4}	1.33×10^{-4}	3.28×10^{-3}
0.187	2.59×10^{-5}	1.30×10^{-4}	1.02×10^{-4}	1.14×10^{-4}	2.80×10^{-3}
0.134	1.86×10^{-5}	1.20×10^{-4}	9.21×10^{-5}	1.05×10^{-4}	2.57×10^{-3}
0.0988	1.37×10^{-5}	1.15×10^{-4}	8.11×10^{-5}	9.55×10^{-5}	2.35×10^{-3}
0.0973	1.35×10^{-5}	1.14×10^{-4}	8.11×10^{-5}	9.52×10^{-5}	2.34×10^{-3}
0.0504	6.98×10^{-6}	1.05×10^{-4}	7.07×10^{-5}	8.43×10^{-5}	2.08×10^{-3}
0.0258	3.58×10^{-6}	1.01×10^{-4}	6.55×10^{-5}	7.94×10^{-5}	1.95×10^{-3}
0.0132	1.83×10^{-6}	9.75×10^{-5}	6.30×10^{-5}	7.65×10^{-5}	1.88×10^{-3}
0.00666	9.23×10^{-7}	9.59×10^{-5}	6.10×10^{-5}	7.46×10^{-5}	1.83×10^{-3}
0	0			7.29×10^{-5}	1.79×10^{-3}

conducting liquid used in this paper, R_0 is 0.232 MΩ.

Tables II–VI show the bubble speed v, capillary number Ca, maximum film thickness h_{max}, minimum film thickness h_{min}, mean film thickness h, and the ratio of film thickness to tube radius h/r. For most of the flow rates, h_{max} and h_{min} were obtained from at least two experiments at the same flow rate. For a stationary bubble the values of h_{max} and h_{min} were obtained for the same bubble at different locations inside the tube. In Table II only one experiment was done for a stationary air bubble of 0.603 cm in length.

The data of Tables II and VI are plotted in Fig. 3 as h/r vs Ca. For comparison two straight lines representing Eqs. [2] and [4] are also plotted.

TABLE III

Experimental Data for Air Bubble, $L = 0.730$ cm

v (cm/s)	Ca	h_{max} (cm)	h_{min} (cm)	h (cm)	$\frac{h}{r}$
0.731	1.01×10^{-4}	2.38×10^{-4}	2.04×10^{-4}	2.18×10^{-4}	5.36×10^{-3}
0.515	7.14×10^{-5}	2.04×10^{-4}	1.63×10^{-4}	1.80×10^{-4}	4.43×10^{-3}
0.411	5.70×10^{-5}	1.60×10^{-4}	1.38×10^{-4}	1.49×10^{-4}	3.68×10^{-3}
0.276	3.82×10^{-5}	1.38×10^{-4}	1.16×10^{-4}	1.25×10^{-4}	3.08×10^{-3}
0.0995	1.38×10^{-5}	1.08×10^{-4}	8.82×10^{-5}	9.75×10^{-5}	2.40×10^{-3}
0.0507	7.03×10^{-6}	9.74×10^{-5}	7.79×10^{-5}	8.66×10^{-5}	2.13×10^{-3}
0.0263	3.64×10^{-6}	9.23×10^{-5}	7.27×10^{-5}	8.16×10^{-5}	2.01×10^{-3}
0.0132	1.83×10^{-6}	8.99×10^{-5}	7.12×10^{-5}	7.93×10^{-5}	1.95×10^{-3}
0.00668	9.26×10^{-7}	8.99×10^{-5}	6.98×10^{-5}	7.88×10^{-5}	1.94×10^{-3}
0.00346	4.79×10^{-7}	8.93×10^{-5}	6.87×10^{-5}	7.75×10^{-5}	1.91×10^{-3}
0.00174	2.41×10^{-7}	8.82×10^{-5}	6.71×10^{-5}	7.62×10^{-5}	1.88×10^{-3}
0	0	7.30×10^{-5}	6.40×10^{-5}	6.95×10^{-5}	1.71×10^{-3}

TABLE IV

Experimental Data for Soltrol 10 Bubble, $L = 0.620$ cm

v (cm/s)	Ca	h_{max} (cm)	h_{min} (cm)	h (cm)	$\frac{h}{r}$
1.95	1.69×10^{-3}	6.33×10^{-4}	5.72×10^{-4}	6.07×10^{-4}	1.49×10^{-2}
1.42	1.23×10^{-3}	5.22×10^{-4}	4.80×10^{-4}	5.04×10^{-4}	1.24×10^{-2}
1.02	8.83×10^{-4}	4.28×10^{-4}	3.99×10^{-4}	4.13×10^{-4}	1.02×10^{-2}
0.727	6.30×10^{-4}	3.63×10^{-4}	3.32×10^{-4}	3.47×10^{-4}	8.54×10^{-3}
0.506	4.38×10^{-4}	2.92×10^{-4}	2.72×10^{-4}	2.83×10^{-4}	6.96×10^{-3}
0.375	3.25×10^{-4}	2.54×10^{-4}	2.30×10^{-4}	2.40×10^{-4}	5.90×10^{-3}
0.264	2.29×10^{-4}	2.10×10^{-4}	1.89×10^{-4}	1.99×10^{-4}	4.90×10^{-3}
0.188	1.63×10^{-4}	1.78×10^{-4}	1.57×10^{-4}	1.67×10^{-4}	4.12×10^{-3}
0.133	1.15×10^{-4}	1.53×10^{-4}	1.31×10^{-4}	1.40×10^{-4}	3.45×10^{-3}
0.0989	8.57×10^{-5}	1.39×10^{-4}	1.14×10^{-4}	1.24×10^{-4}	3.06×10^{-3}
0.0977	8.46×10^{-5}	1.37×10^{-4}	1.12×10^{-4}	1.23×10^{-4}	3.02×10^{-3}
0.0505	4.37×10^{-5}	1.17×10^{-4}	8.64×10^{-5}	1.00×10^{-4}	2.46×10^{-3}
0.0259	2.24×10^{-5}	1.05×10^{-4}	7.35×10^{-5}	8.64×10^{-5}	2.12×10^{-3}
0.0132	1.14×10^{-5}	1.01×10^{-4}	6.87×10^{-5}	8.16×10^{-5}	2.01×10^{-3}
0.00669	5.79×10^{-6}	9.85×10^{-5}	6.37×10^{-5}	7.74×10^{-5}	1.90×10^{-3}
0	0	7.40×10^{-5}	6.97×10^{-5}	7.18×10^{-5}	1.77×10^{-3}

From these results we conclude the following.

(a) For both air and oil cases, the wetting film thickness decreases with decreasing bubble speed and approaches a constant value of about 0.7 μm when the bubble is stationary, as shown in Tables II–VI. Measurements were also made for a stationary air bubble of 2.0

TABLE V

Experimental Data for Soltrol 100 Bubble, $L = 0.626$ cm

v (cm/s)	Ca	h_{max} (cm)	h_{min} (cm)	h (cm)	$\frac{h}{r}$
2.06	1.89×10^{-3}	6.64×10^{-4}	6.04×10^{-4}	6.33×10^{-4}	1.56×10^{-2}
1.39	1.27×10^{-3}	5.54×10^{-4}	4.93×10^{-4}	5.23×10^{-4}	1.29×10^{-2}
1.02	9.33×10^{-4}	4.66×10^{-4}	4.22×10^{-4}	4.44×10^{-4}	1.09×10^{-2}
0.702	6.42×10^{-4}	3.84×10^{-4}	3.46×10^{-4}	3.64×10^{-4}	8.96×10^{-3}
0.510	4.67×10^{-4}	3.27×10^{-4}	2.84×10^{-4}	3.04×10^{-4}	7.49×10^{-3}
0.363	3.32×10^{-4}	2.68×10^{-4}	2.32×10^{-4}	2.49×10^{-4}	6.12×10^{-3}
0.261	2.39×10^{-4}	2.41×10^{-4}	1.96×10^{-4}	2.14×10^{-4}	5.27×10^{-3}
0.182	1.67×10^{-4}	1.83×10^{-4}	1.61×10^{-4}	1.71×10^{-4}	4.22×10^{-3}
0.131	1.20×10^{-4}	1.54×10^{-4}	1.37×10^{-4}	1.45×10^{-4}	3.58×10^{-3}
0.0943	8.63×10^{-5}	1.36×10^{-4}	1.18×10^{-4}	1.26×10^{-4}	3.10×10^{-3}
0.0993	9.09×10^{-5}	1.36×10^{-4}	1.21×10^{-4}	1.28×10^{-4}	3.14×10^{-3}
0.0507	4.64×10^{-5}	1.14×10^{-4}	9.49×10^{-5}	1.03×10^{-4}	2.55×10^{-3}
0.0260	2.38×10^{-5}	1.02×10^{-4}	8.35×10^{-5}	9.18×10^{-5}	2.26×10^{-3}
0.0132	1.21×10^{-5}	9.65×10^{-5}	7.80×10^{-5}	8.62×10^{-5}	2.12×10^{-3}
0.00680	6.22×10^{-6}	9.31×10^{-5}	7.47×10^{-5}	8.28×10^{-5}	2.04×10^{-3}
0.00174	1.59×10^{-6}	9.00×10^{-5}	7.08×10^{-5}	7.92×10^{-5}	1.95×10^{-3}
0	0	7.67×10^{-5}	7.08×10^{-5}	7.36×10^{-5}	1.81×10^{-3}

TABLE VI

Experimental Data for Soltrol 220 Bubble, $L = 0.643$ cm

v (cm/s)	Ca	h_{max} (cm)	h_{min} (cm)	h (cm)	$\frac{h}{r}$
1.99	1.68×10^{-3}	6.39×10^{-4}	5.96×10^{-4}	6.17×10^{-4}	1.52×10^{-2}
1.42	1.20×10^{-3}	5.32×10^{-4}	5.00×10^{-4}	5.14×10^{-4}	1.27×10^{-2}
1.01	8.52×10^{-4}	4.62×10^{-4}	4.27×10^{-4}	4.42×10^{-4}	1.09×10^{-2}
0.719	6.07×10^{-4}	3.81×10^{-4}	3.36×10^{-4}	3.57×10^{-4}	8.78×10^{-3}
0.520	4.39×10^{-4}	3.25×10^{-4}	2.86×10^{-4}	3.05×10^{-4}	7.52×10^{-3}
0.368	3.13×10^{-4}	2.61×10^{-4}	2.31×10^{-4}	2.47×10^{-4}	6.07×10^{-3}
0.268	2.26×10^{-4}	2.20×10^{-4}	1.94×10^{-4}	2.07×10^{-4}	5.09×10^{-3}
0.185	1.56×10^{-4}	1.85×10^{-4}	1.63×10^{-4}	1.74×10^{-4}	4.27×10^{-3}
0.136	1.15×10^{-4}	1.62×10^{-4}	1.42×10^{-4}	1.51×10^{-4}	3.73×10^{-3}
0.0995	8.39×10^{-5}	1.44×10^{-4}	1.24×10^{-4}	1.33×10^{-4}	3.27×10^{-3}
0.0960	8.10×10^{-5}	1.44×10^{-4}	1.20×10^{-4}	1.32×10^{-4}	3.25×10^{-3}
0.0504	4.25×10^{-5}	1.22×10^{-4}	1.01×10^{-4}	1.10×10^{-4}	2.71×10^{-3}
0.0259	2.19×10^{-5}	1.12×10^{-4}	8.98×10^{-5}	9.98×10^{-5}	2.46×10^{-3}
0.0136	1.15×10^{-5}	1.07×10^{-4}	8.36×10^{-5}	9.37×10^{-5}	2.31×10^{-3}
0.00670	5.65×10^{-6}	1.04×10^{-4}	8.01×10^{-5}	9.03×10^{-5}	2.22×10^{-3}
0.00178	1.50×10^{-6}	9.97×10^{-5}	7.66×10^{-5}	8.66×10^{-5}	2.13×10^{-3}
0	0	7.92×10^{-5}	7.31×10^{-5}	7.60×10^{-5}	1.87×10^{-3}

cm in length in another tube from the same batch and the apparent film thicknesses were 0.61 and 0.64 μm at two different locations.

The leveling off of the film thickness to an equilibrium value for decreasing Ca was predicted by Teletzke (16) for a nonwetting fluid displacing a perfectly wetting fluid in an ideally smooth circular tube. For large Ca his prediction was the same as Bretherton's. Both Eqs. [2] and [4] predict zero film thickness for a stationary bubble, whereas Eq. [3] predicts a negative film thickness.

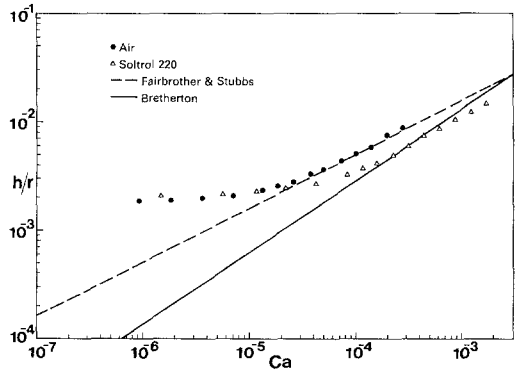

FIG. 3. h/r as a function of Ca. (●) Data for air bubble, (△) data for Soltrol 220 bubble, (---) Fairbrother and Stubbs, (—) Bretherton.

In cases where the film thickness is smaller than about 0.1 μm, colloidal forces should be taken into account. Since these forces are responsible for the film stability and the wettability of the system at hand (see, for example, (2, 16–18)). To illustrate the effect of one of these forces, let us estimate the equilibrium film thickness h_e surrounding a long stationary bubble inside an idealized tube. At equilibrium the difference between the capillary pressure in the film and at the end of the bubble, γ/r, must be balanced by the positive disjoining pressure in the film. Here we assume a retarded van der Waals disjoining pressure $-B/h^4$, with $B = -10^{-19}$ erg cm. For an air bubble surrounded by the same liquid in a perfectly smooth and circular tube of the same radius as in the experiment, the equilibrium film thickness h_e is

$$h_e = \left(\frac{-Br}{\gamma}\right)^{1/4} \approx 3 \times 10^{-6} \text{ cm}. \quad [6]$$

A similar estimate can be made using a nonretarded van der Waals disjoining pressure, $-B/h^3$, with B of the order of -10^{-14} erg. The fact that the measured film thickness (0.7 μm), is one order of magnitude larger than the calculated value is consistent with the axially directed grooves described above. At equilibrium most of the wetting liquid is in these grooves, where most of the electrical current is conducting, because the capillary pressure is not large enough to squeeze the liquid out of the grooves, whose width are less than 10 μm.

(b) For an air bubble moving with a value of Ca ranging between 5.02×10^{-5} and 2.74×10^{-4}, the measured wetting film thickness (from 1.51 to 3.61 μm) correlates with Eq. [2], as shown in Fig. 3.

This equation was established empirically by Fairbrother and Stubbs (10) for film thicknesses range from 6 to 73 μm. In experiments of Taylor (11) and Goldsmith and Mason (15), the film thicknesses measured were larger than 6 μm. Unfortunately, due to the imperfection of the tube, we were unable to investigate the film of 0.1 to 1 μm thick. The measured film thickness of less than a micrometer reported here should be looked at as a result of the effects of the roughness.

The reason why the data agree with Eq. [2] rather than Eq. [4] is not clear. In deriving Eq. [2], the film was assumed to be at rest relative to the tube (10). This has been substantiated in Goldsmith and Mason's experiments (15) for a narrow range of capillary number, $0.013 < Ca < 0.09$. Bretherton (14) predicted that the film thickness would be smaller by a factor of $2^{-1/3}$ for a rigid fluid–fluid interface

$$\frac{h}{r} = 1.06Ca^{2/3} \qquad [7]$$

than that given by Eq. [4] for a mobile interface. It is obvious that Eq. [7] gives a worse prediction. This is puzzling since we do not expect the fluids to be perfectly clean to ensure a mobile interface.

(c) For an oil bubble moving with a value of Ca ranging between $\approx 2 \times 10^{-4}$ and 2×10^{-3}, the data agree better with Eq. [4] than with Eq. [2]. For this range of Ca, the measured film thickness varies between 2 and 6 μm.

(d) There is no appreciable difference in the film thickness for the different oils with varying viscosity for all Ca, but the thickness is smaller than that for an air bubble moving at the same $Ca > 10^{-5}$. Probably the range of the viscosity ratio of oil to water investigated is not large enough to see the difference in h. The reason for the smaller thickness for an oil bubble than for an air bubble is not clear to the author, although the adsorption of the dye at the oil–water interface is a possibility (see discussion in (b)). The data do not agree with Teletzke's (16) theory which predicts an increase in film thickness with an increase in viscosity ratio μ_b/μ_c.

The data reported here indicate that at equilibrium the surface roughness is important in wetting film distribution and in electrical conduction. The effect of roughness should be stronger in smaller capillaries. In porous rocks the situation is more complicated because the wetting liquid can be distributed both on the surface and in between the grains. The proportion of distribution depends on the pore structure, surface roughness, and saturation of the wetting liquid. But for low wetting phase saturation, the surface roughness effects should become more important.

ACKNOWLEDGMENTS

I would like to thank B. Schmidt for her assistance with experiments, A. Surcheck for making the Plexiglas chambers, L. McGowan and C. Straley for taking the SEM micrograph, and E. B. Dussan V. for her comments on an earlier version of this paper.

REFERENCES

1. Roof, J. G., *Soc. Pet. Eng. J.* **10,** 85 (1970).
2. Mohanty, K. K., "Fluids in Porous Media: Two-Phase Distribution and Flow," Ph.D. thesis. Department of Chemical Engineering, University of Minnesota, 1981.
3. Arriola, A., Willhite, G. P., and Green, D. W., *Soc. Pet. Eng. J.* **23,** 99 (1983).

4. Chen, J. D., and Koplik, J., *J. Colloid Interface Sci.* **108,** 304 (1985).
5. Wardlaw, N. C., *J. Canad. Pet. Technol.* **21,** 21 (1982).
6. Chatzis, I., Morrow, N. R., and Lim, H. T., *Soc. Pet. Eng. J.* **23,** 311 (1983).
7. Keller, G. V., *Oil Gas J.* **51,** 62 (1953).
8. Sweeney, S. A., and Jennings, H. Y., *Prod. Mon.* **24,** 29 (1960).
9. Mungan, N., and Moore, E. J., *J. Canad. Pet. Technol.* **7,** 20 (1968).
10. Fairbrother, F., and Stubbs, A. E., *J. Chem. Soc.* **1,** 527 (1935).
11. Taylor, G. I., *J. Fluid Mech.* **10,** 161 (1961).
12. Kussakov, M. M., and Mekenitskaya, L. I., *in* "Proceedings, 4th World Petroleum Congress," Sec. II, p. 593 (1955).
13. Marchessault, R. N., and Mason, S. G., *Ind. Eng. Chem.* **52**(1), 79 (1960).
14. Bretherton, F. P., *J. Fluid Mech.* **10,** 166 (1961).
15. Goldsmith, H. L., and Mason, S. G., *J. Colloid Sci.* **18,** 237 (1963).
16. Teletzke, G. F., "Thin Liquid Film," Ph.D. thesis. Department of Chemical Engineering, University of Minnesota, 1983.
17. Chen, J. D., *J. Colloid Interface Sci.* **98,** 329 (1984).
18. Melrose, J. C., "Interpretation of Mixed Wettability States in Reservoir Rocks," SPE paper 10971, Soc. Pet. Eng., 6200 N. Central Expressway, P.O. Drawer 64706, Dallas, TX 75206 (1982).